

## BL20B2

### Medical and Imaging I

#### 1. Introduction

BL20B2 is a medium-length beamline with a bending magnet source. It is composed of an optics hutch (OH), upstream experimental hutch 1 (EH1) located 42 m from the source, and downstream experimental hutches 2 (EH2) and 3 (EH3) located more than 200 m from the source. EH2 and EH3 are located in Medium-Length Beamline Facility. A monochromatic X-ray beam from a SPring-8 standard double-crystal monochromator is available. The energy ranges from 5 keV to 113 keV can be covered by changing the net plane of the monochromator.

BL20B2 is mainly used for X-ray imaging techniques such as X-ray microtomography and real-time radiography. In EH1, high-spatial-resolution and fast-imaging experiments, which require a high photon flux density, are performed. In comparison, X-ray imaging experiments with a wide field of view are performed in EH2 and EH3 using an X-ray beam with a large cross section. In addition, phase contrast imaging based on a high spatial coherence of the beam generated over a long propagation distance from the source is also performed. As the activities in FY2020, X-ray phase tomography using a grating interferometer was upgraded. In addition, a double-bounce multilayer monochromator (DMM) was installed at OH as a new optical system.

#### 2. Upgrade of X-ray phase tomography

X-ray phase tomography makes it possible to measure biological soft tissues with a higher image contrast than in the case of conventional absorption-

based X-ray microtomography [1]. In addition, quantitative measurements such as three-dimensional densitometry can be carried out to reveal the biological functions of tissues. As reported in the FY2018 annual report, a new grating interferometer was introduced in X-ray phase tomography at EH1 to improve the spatial resolution [2]. Then, it was confirmed that the new grating interferometer could be applied to the high-resolution X-ray phase tomography of biological samples.

As an upgrade of X-ray phase tomography at EH1, a dedicated sample stage including an optimized sample holder and a general-purpose high-definition CMOS camera for an X-ray imaging detector were introduced. Then, an X-ray phase tomography system combined with the grating interferometer that was already installed in FY2018 was developed. A dedicated sample stage for X-ray phase tomography is shown in Fig. 1(a). A strong frame supports a high-precision rotation stage,

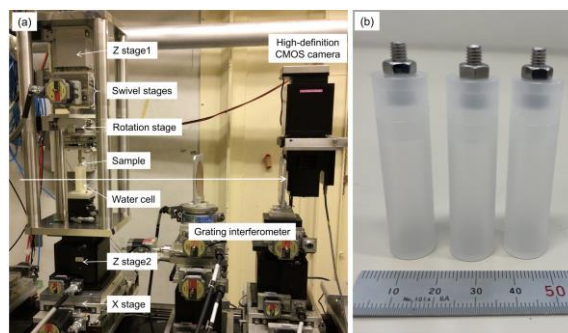


Fig. 1. (a) Exterior of X-ray phase tomography system at EH1. (b) Optimized sample holders for X-ray phase tomography at EH1.

swivel stages for axial alignment, and a vertical translation stage to measure the sample in water. As a consequence, the sample set in the holder can be rotated in a specially designed water cell. In this system, a cylindrical sample holder was also optimized to fit the effective field of view of the system. The effective field of view in the slice image obtained from a tomographic measurement is basically determined by the horizontal field of view in the projection image. The horizontal field of view in X-ray phase tomography depends on the X-ray imaging detector as in other imaging experiments. To keep the effective pixel size small and the effective field of view wide, a general-purpose high-definition CMOS camera (C13949-50U, Hamamatsu Photonics) was introduced. Since the effective field of view in the X-ray imaging detector is expressed as the product of the effective pixel size and the number of pixels, the high-definition CMOS camera is appropriate for such an observation. This high-definition CMOS camera was used in a lens-coupled visible-light-conversion-type X-ray imaging detector. As a phosphor screen for converting an X-ray image into a visible-light image, a powder-type  $\text{Gd}_2\text{O}_2\text{S}:\text{Tb}^+$  scintillator with a thickness of 15  $\mu\text{m}$  was used. The effective pixel size and horizontal field of view were 3.46  $\mu\text{m}$  and 14.2 mm, respectively. Therefore, the outer diameter of the sample holder was determined to be 13 mm so that the entire sample including the holder should fit into the horizontal field of view. A photo of the sample holder is shown in Fig. 1(b). To maintain the inner volume as much as possible, the wall thickness was set to 0.5 mm. Polypropylene, which has a lower density than water and is easy to fabricate, was selected as the holder material. In addition, the thickness of the water cell along the

optical axis was set to 15 mm to accommodate the outer diameter of the sample holder and minimize the X-ray absorption by water. As a demonstration of X-ray phase tomography using the upgraded system, a formalin-fixed mouse embryo (E14) was observed. A sectional image of the embryo is shown in Fig. 2. The outer diameter of the sample holder matches the reconstructed field of view. In addition, the detailed internal structure of the whole body of the embryo can be observed owing to the high-definition CMOS camera.

On the other hand, the X-ray phase tomography system at EH2 for the observation of large samples was also upgraded by introducing a new grating interferometer and a fiber-coupled high-definition sCMOS camera (C15606-SY73177, Hamamatsu Photonics). The new gratings with a grating period of 2.4  $\mu\text{m}$  were produced by

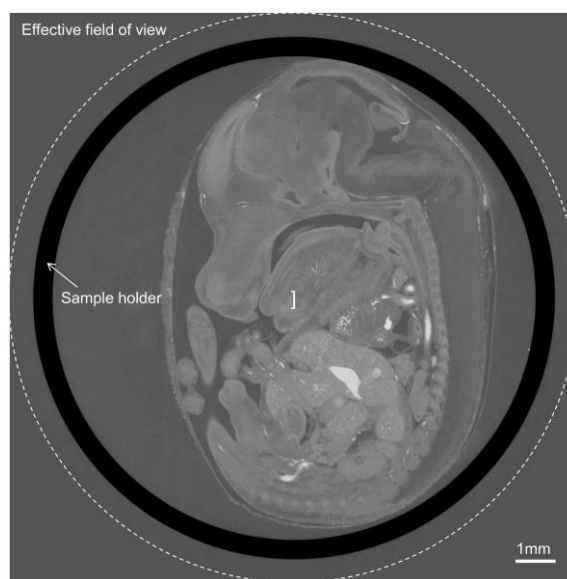


Fig. 2. X-ray phase tomographic image of a formalin-fixed mouse embryo. The embryo set in the holder was fixed with 1% agarose gel. The X-ray energy was 20 keV. 1800 projections, 500 ms exposure, and 5-step fringe scan.

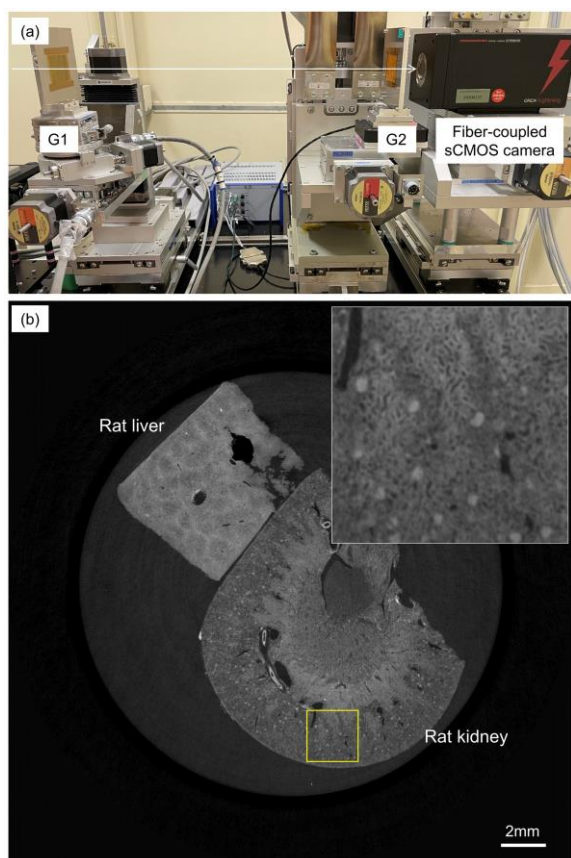


Fig. 3. (a) Exterior of new gratings and fiber-coupled high-definition sCMOS camera. (b) X-ray phase tomographic image of formalin-fixed rat kidney and liver. The inset shows a magnified image of the square region. X-ray energy: 25 keV. 1800 projections, 500 ms exposure, and 5-step fringe scan.

GratXray in Switzerland<sup>[3]</sup>. A phase grating (G1) is optimized to generate  $\pi/2$  shift at the X-ray energy of 25 keV. An absorption grating (G2) is made of gold with a pattern thickness of 40.7  $\mu\text{m}$ . A smaller grating period is advantageous for high-spatial-resolution observation<sup>[4]</sup>. The fiber-coupled sCMOS camera has a straight optical fiber to transmit the visible light image generated at the scintillator to the image sensor. The diameter of the

optical fiber is 6  $\mu\text{m}$ , and a powder-type  $\text{Gd}_2\text{O}_2\text{S:Tb}^+$  scintillator with a thickness of 15  $\mu\text{m}$  is combined with the optical fiber. The effective pixel size and the field of view of this camera are 5.5  $\mu\text{m}$  and 25.3 (H) mm  $\times$  14.3 (V) mm, respectively. A photo of the upgraded X-ray phase tomography system at EH2 is shown in Fig. 3(a). The distance between G1 and G2 was set to a 9/2-order fractional Talbot distance, that is, 523 mm. The average visibility in the Moiré pattern generated by G1 and G2 at a 9/2-order fractional Talbot distance was 49%. As a demonstration of X-ray phase tomography, formalin-fixed rat kidney and liver samples were observed. Cross sections of the samples are shown in Fig. 3(b). Biological samples could be measured with less than half the effective pixel size compared with previous measurements and the total measurement time was almost the same as before.

### 3. Installation of double-bounce multilayer monochromator (DMM)

As an upgrade of the beamline optical system, two kinds of DMM were introduced in order to increase the X-ray photon flux density at X-ray energies of 40 keV and 110 keV. As shown in Fig. 4, the first elements (M1a and M1b) in DMM are arranged in tandem along the optical axis. In comparison, the second elements (M2a/b) are installed in the same vacuum chamber. M2a and M2b can be switched by horizontal translation across the optical axis. Each DMM has a W/B<sub>4</sub>C coat on the silicon substrate. The photon flux density is expected to increase by a factor of more than 100 at 40 keV and 110 keV. In addition to the newly installed DMM, an existing double-crystal monochromator is also available. Other optical devices were also rearranged to use

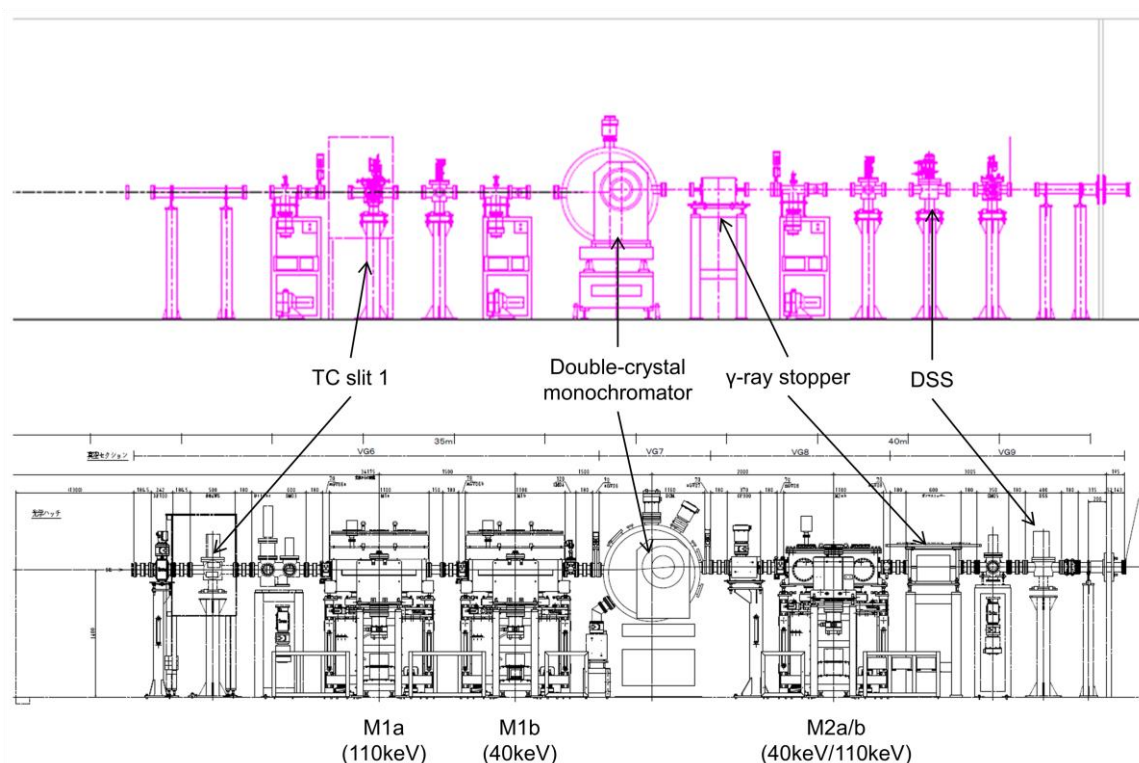


Fig. 4. Schematic drawing of the optical components in OH before (upper) and after (lower) installation of DMM.

the double-crystal monochromator and DMM as shown in Fig. 4.

#### 4. Conclusion

X-ray phase tomography systems at EH1 for high-spatial-resolution observation and at EH2 for the observation of large samples were upgraded. Compared with previous measurements, the performance of these systems was improved in terms of spatial resolution, stability, and ease of measurements. On the other hand, the amount of data has become enormous owing to the introduction of high-definition cameras. Therefore, handling large amounts of data will be an issue for the future.

Two kinds of DMM for 40 keV and 110 keV pink beams were installed at OH as a new optical

component of the beamline. Performance evaluation will be conducted in the future.

Masato Hoshino and Kentaro Uesugi

Spectroscopy and Imaging Division, Center for Synchrotron Radiation Research, JASRI

#### References:

- [1] Momose, A. (2005). *Jpn. J. Appl. Phys.* **44**, 6355–6367.
- [2] Hoshino, M. & Uesugi, K. (2019). *Spring-8/SACLA Annual Report FY2018*, 49–51.
- [3] <https://www.gratxray.com/>
- [4] Weitkamp, T. Diaz, A. David, C. Pfeiffer, F. Stambanoni, M. Cloetens, P. & Ziegler, E. (2005). *Opt. Express* **13**, 6296–6304.